Analysis and Design of Broad-Band Single-Layer Rectangular U-Slot Microstrip Patch Antennas

Steven Weigand, *Member, IEEE*, Greg H. Huff, Kankan H. Pan, and Jennifer T. Bernhard, *Senior Member, IEEE*

***Abstract*—A wide operating bandwidth for a single-layer coaxially fed rectangular microstrip patch antenna can be obtained by cutting a U-shaped slot on the patch. This antenna structure has recently been found experimentally to provide impedance bandwidths of 10%–40%, even with nonair substrates. However, design rules for this antenna have not yet been presented. This paper develops principle design procedures through examination of the structure's multiple resonant frequencies as well as the radiation and impedance properties of different antenna geometries. The approximate design rules are derived by analysis of former experiments, method of moments (MoM) simulations, and measurement results. Simulations and measurements of several antennas designed using these new rules are presented and directions for further study are discussed.**

***Index Terms*—Broad-band antenna, microstrip antenna, U-slot antenna.**

I. Introduction

In RECENT years, the demand for broad-band antennas has increased for use in high-frequency and high-speed data communication. Printed antennas are economical and easily hidden inside packages, making them well suited for consumer applications. Unfortunately, a "classical" microstrip patch antenna has a very narrow frequency bandwidth that precludes its use in typical communication systems. However, if the frequency bandwidth could be widened, a broad-band microstrip antenna would prove very useful in commercial applications such as 2.5 G and 3 G wireless systems, wireless local area networks (WLAN), and Bluetooth personal networks.

Researchers have devised several methods to increase the bandwidth of microstrip antennas in addition to the common techniques of increasing patch height and decreasing substrate permittivity. These include using a multilayer structure consisting of several parasitic radiating elements with slightly different sizes above the driven element (a stacked patch antenna) [1] or a planar patch antenna surrounded by closely spaced parasitic patches (a coplanar parasitic subarray) [2]. The stacked patch antenna increases the thickness of the antenna while the coplanar geometry increases the lateral size of the antenna. Incorporation of a dissipative load in a single-layer single-patch antenna through addition of high loss material or resistors also increases bandwidth but compromises the antenna's efficiency and gain [3], [4]. The bandwidths of single patch antennas can also be increased by implementing internal structures such as shorting pins [5], [6] or slots [7].

In 1995, Huynh and Lee [7] presented an experimental study of a new kind of broad-band antenna with an impedance bandwidth of 47%. The new antenna was a probe-fed rectangular microstrip patch antenna on a unity permittivity substrate with an internal U-shaped slot as shown in Fig. 1 [7]. Since then, a number of experimental and theoretical papers have been presented for this antenna [8]–[24]. None of these papers, however, provide detailed parametric studies or design models that permit *a priori* designs. Some of the conclusions from these papers actually contradict each other, making the design process more confusing. Recently, researchers have proposed a similar design on a microwave substrate [24].

In this paper, we present a set of simple design procedures for the rectangular U-slot microstrip patch antenna on microwave substrates. These procedures provide antenna engineers with approximate rules that result in a good first-pass design with prescribed characteristics that requires only minimal tuning. Additionally, the accompanying parametric studies give direction for the selection and variation of the proper geometric and material parameters to achieve desired antenna behavior. The next section details the parametric studies used to develop the design procedure. Section III outlines the design procedure that draws from the results of the parametric studies as well as the work of previous investigators. Section IV provides several designs as examples and illustrates the use of the parametric studies' results for the tuning process. Finally, Section V discusses the results obtainable with these design rules as well as their limitations and outlines directions for future research on this antenna structure.

II. Parametric Studies

In this paper, we first analyze the behavior of the antenna using its resonant frequencies and then examine the VSWR and 2 : 1 VSWR bandwidth of each configuration during the tuning process. Several previous studies (e.g., [7], [8]) look mainly at minimum VSWR frequencies or bandwidth, which may not correspond to resonant conditions or provide much insight into antenna operation. Others (e.g., [9], [23]) consider only some of the resonant frequencies. Additionally, former studies assert that the antenna's broad-band characteristics are the result of reactive cancellation between the capacitive U-slot and the inductive probe feed and/or the currents around the U-slot [7], [11].

Manuscript received May 5, 2001; revised February 13, 2002.

S. Weigand was with the Technical University of Darmstadt, Darmstadt, Germany. He is now with WJ Communications, San Jose, CA 95134 USA.

G. H. Huff and J. T. Bernhard are with the Electromagnetics Laboratory, Department of Electrical and Computer Engineering, University of Illinois at Urbana-Champaign, Urbana, IL 61801 USA.

K. H. Pan was with the Electromagnetics Laboratory, Department of Electrical and Computer Engineering, University of Illinois at Urbana-Champaign. She is now with Agilent Technologies, Santa Rosa, CA 95403 USA.

Digital Object Identifier 10.1109/TAP.2003.809836

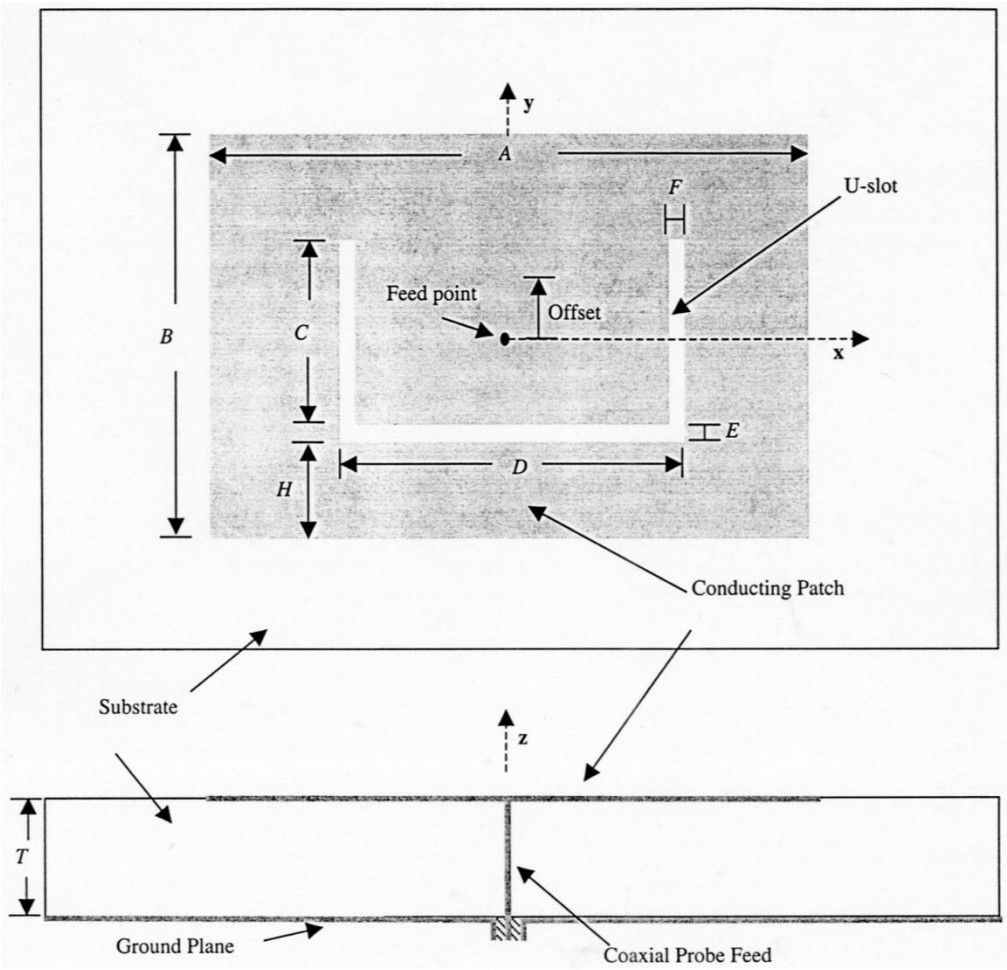

Fig. 1. Geometry of the rectangular U-slot microstrip patch antenna.

TABLE I
DIMENSIONS AND MATERIAL PROPERTIES OF THE INITIAL U-SLOT ANTENNA USED IN THE PARAMETRIC STUDIES

A [mm]	B [mm]	C [mm]	D [mm]	E [mm]	F [mm]	H [mm]	R [mm]	T [mm]	Offset [mm]	ε_r
36.0	26.0	12.0	16.0	2.0	2.0	4.0	0.5	5.0	0.0	2.20

This explanation, however, does not capture the complex relationships between antenna geometries and characteristics, since alterations of parameters such as the width and length of the U-slot, the height and size of the patch, the substrate permittivity, and the probe radius and position can dramatically change the antenna's behavior.

The antenna geometry provided in [7] served as the basis for the parametric studies, which were carried out using a method of moments simulation package (IE3D) [25]. Since it is difficult to achieve repeatable construction using foam substrates, we scaled the original design to reside on a substrate with a relative permittivity equal to 2.2. The initial geometric and material parameters are provided in Table I. Using the common formulas found in [26], the simple patch (without U-slot) with the initial length and width listed in Table I has a TM_{01} mode resonant frequency of approximately 3.44 GHz and a TM_{20} mode resonant frequency of approximately 5.27 GHz. For ease of reference, the patch edges are indicated by their position in Fig. 1, that is, Vertical Left, Vertical Right, Horizontal Top, Horizontal Bottom. The U-slot is discussed in terms of its base (of length D) and its vertical arms (of length C). The copolar and cross-polar field directions are defined in terms of the fields of a plain microstrip patch antenna with length B (~half wavelength) and width $A(B < A)$.

With the addition of the U-slot at the location specified in Table I, the impedance bandwidth (defined by 2 : 1 VSWR) is 9% with a center frequency of approximately 4 GHz. The input impedance of this antenna over frequency (Fig. 2) shows four resonances (defined by purely real input impedances) created as a result of the double loop characteristic pointed out in [7].

In the parametric studies, only one parameter was changed at a time and all parameters not specified remained at the values given in Table I. The dimensions and positions of the U-slot were varied first. C was varied from 0 to 18 mm in 2-mm steps with D equal to 16 mm. D was varied from 6 to 22 mm in 2-mm steps with C equal to 12 mm. E and F, the width of the U-slot in

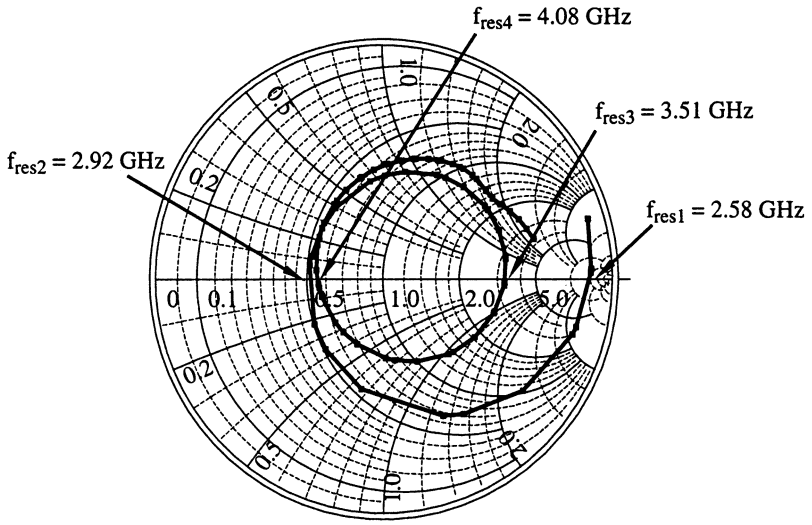

Fig. 2. Simulated input impedance of the initial U-slot microstrip patch antenna used in the parametric studies. The four resonant frequencies of the structure are indicated.

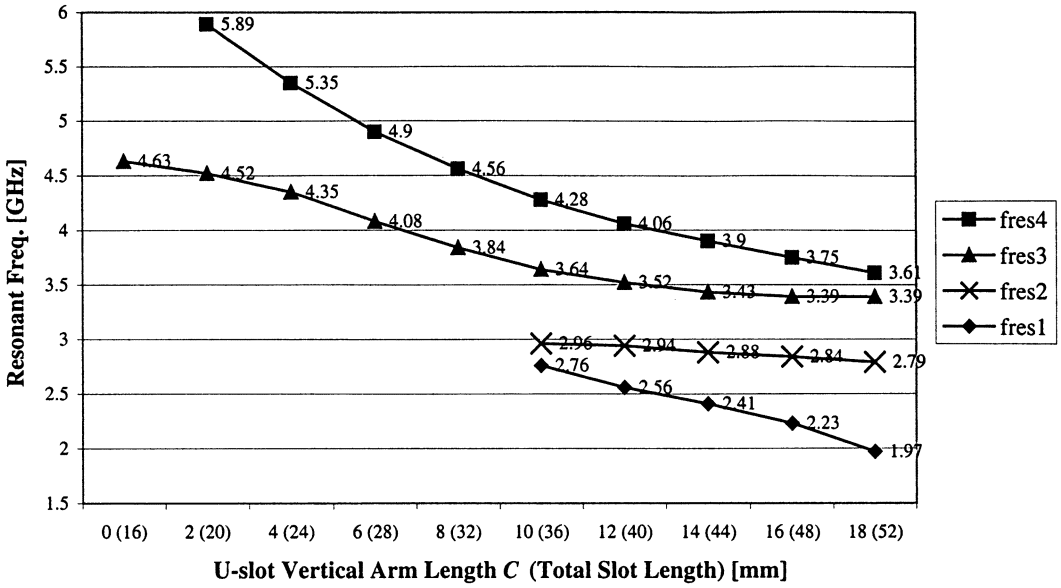

Fig. 3. Parametric study results for variations in U-slot vertical arm length C.

the two dimensions, were varied between 0.5–2 mm with equal and unequal values, i.e., $(E,\ F) = (0.5\text{ mm}, 0.5\text{ mm})$, (0.5 mm, 2.0 mm), (2.0 mm, 0.5 mm), and (2.0 mm, 2.0 mm). The slot gap widths E and F are modified in such a way that only the outer part of the "U" is trimmed or expanded. Finally, the slot position designated by H was varied from 2 to 6 mm. Next, parameters of the patch itself were changed. These included variations in A from 36 to 54 mm, B from 20 to 32 mm, and patch height T from 3 to 7 mm. The probe radius R was varied from 0.3 to 1.3 mm and the substrate's relative permittivity was varied from 1.0 to 2.9. The feed point is always at the center of the patch and the U-slot is always centered in the x-dimension of the patch. While these parametric studies are not exhaustive, they do provide a number of insights into the antenna's behavior that have been exploited in the design procedure developed in Section III. These observations may also be used in subsequent design studies.

The parametric study results are based on an antenna design where four resonances occur as defined by $jX = 0$ axis crossings on the Smith chart. Some antenna configurations in the study did not possess the double loop characteristic and therefore did not have four resonances according to this definition. In these cases, we assumed the continuation of trends established by other data to designate certain frequencies as related to the first, second, third, or fourth resonances.

A. Analysis of the Resonant Frequencies

Since the currents on the patch surface cannot be separated into pure modes of either the slot or the patch, each parameter variation necessarily causes some changes in all of the resonant frequencies. However, some of these changes are larger and more pronounced than others, which leads to hypotheses about the relationships between geometry and behavior. This section explores these relationships.

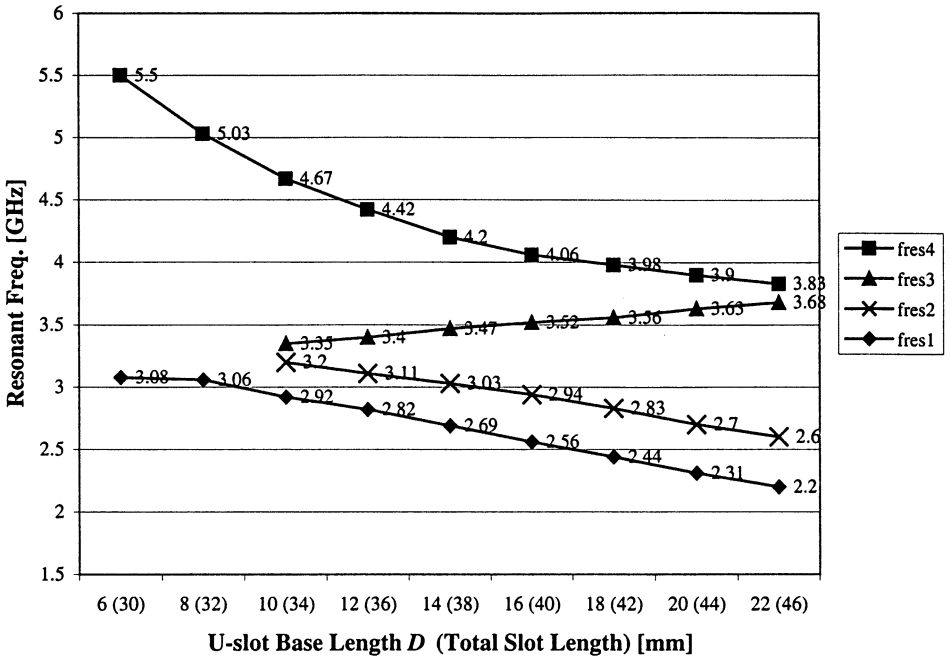

Fig. 4. Parametric study results for variations in U-slot base length D.

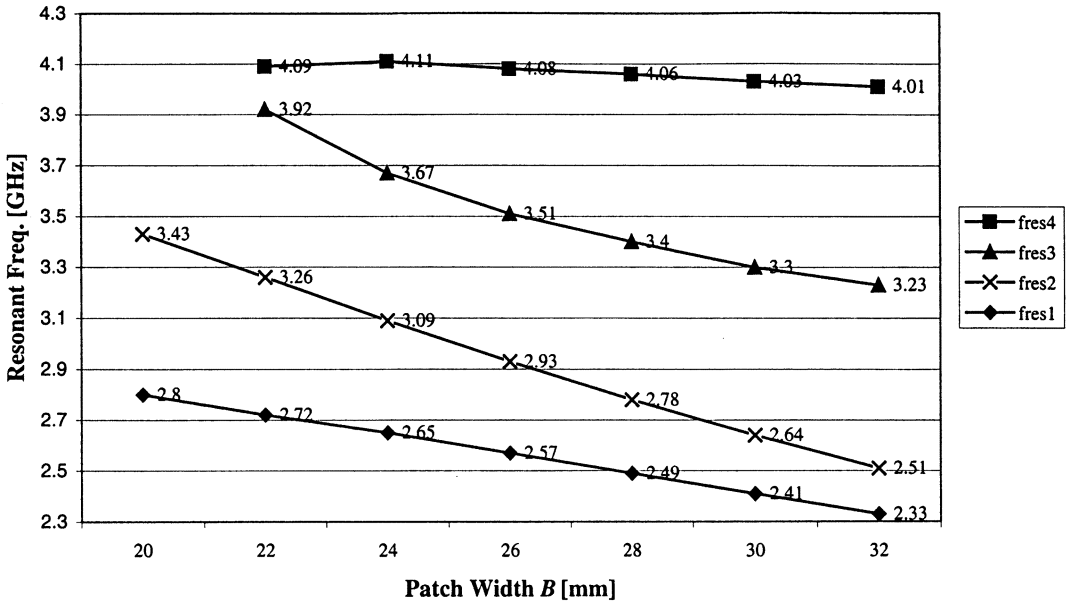

Fig. 5. Parametric study results for variations in patch width B.

The First Resonance f_{res1}: The first resonant frequency appears to be dominated by the first slot resonance in the dielectric substrate. Since the input impedance of the resonance is very high, however, it does not radiate well. As indicated by the data presented in Figs. 3 and 4, the first resonant frequency changes linearly with the total slot length approximated by the value of $2C + D$, neglecting corners. Note that the normalized value of the total slot length to resonant frequency wavelength remains very stable as the slot dimensions are changed. For instance, with $C = 18$ mm and $D = 16$ cm, the total slot length is approximately 52 mm. In the substrate with relative permittivity of 2.2, this length corresponds to a half wavelength at a resonant frequency of 1.94 GHz. Likewise, with $C = 12$ mm and $D = 20$ mm, the total slot length is approximately 44 mm, which corresponds to a resonant frequency of 2.33 GHz. An-

TABLE II
VARIATIONS OF f_{res1} WITH CHANGES IN SUBSTRATE PERMITTIVITY WITH ALL OTHER ANTENNA PARAMETERS REMAINING AT THE VALUES GIVEN IN TABLE I. THE PREDICTED VALUE OF f_{res1} IS CALCULATED BY ASSUMING THAT THE VALUE OF $2C + D$ IS A HALF WAVELENGTH IN THE SUBSTRATE MATERIAL

ε_r	f_{res1} [GHz]	f_{res1} (predicted) [GHz]	% Difference
1.0	3.42	3.75	9.6
1.5	2.97	3.06	3.0
2.2	2.57	2.53	-1.6
2.9	2.30	2.20	-4.3

TABLE III
SUMMARY OF PARAMETRIC STUDY RESULTS FOR INCREASES IN GEOMETRICAL AND MATERIAL PARAMETERS

	A+	B+	C+	D+	E+	F+	H+	ε_r+	T+	R+	Offset+
f_{res1}	0	–	–	–	+	–	0(–)	–	0	0(–)	0
f_{res2}	0	–	0(–)	–	+	–	0(–)	–	0(–)	0(+)	0
f_{res3}	–*	–	–*	0(+)	0	0	0	–	–	0(–)	+
f_{res4}	–	0	–	–	+	–	+	–	–	+	–
Δf_{12}	0	–	+	0	0	+	0	0(-)	–	+	0
Δf_{23}	–	0	0	+	–	+	0	0	–	–	+
Δf_{34}	0	+	–	–	+	–	+	0	0	+	–
Δf_{24}	–	+	–	0	+	0	+	0	–	+	–
Δf_{14}	–	0(+)	0	0	+	+	+	0	–	+	–
$\lvert \Delta f_{34} - \Delta f_{23} \rvert$	+	–	+	v	–	–	0	0	0	v	v
$VSWR_2$	–	–	+	+	–	+	+	+	–	0	+
$VSWR_3$	–	+	–	–	+	–	+	+	+	–	–
$VSWR_4$	0	+	0	–	+	–	0	+	–	+	–
$\Delta VSWR_{23}$	–	+	-	–	+	–	+	^	v	–	v
$\Delta VSWR_{34}$	0(^)	+	v	v	+	–	+	+	v	–	–
$\Delta VSWR_{24}$	+	0(v)	+	v	–	–	+	–	–	0	+

other indication that this is a slot-dominated mode comes from the data in Table II, which shows four points over a variation of the relative permittivity of the substrate with $C = 12$ mm and $D = 16$ mm. The deviations away from the half wavelength approximation as permittivity changes may be caused by accompanying changes in the apparent width of the slot, which may shift the resonant frequency slightly. The resonant frequency also changes with B as shown in Fig. 5, but with about half as much effect as a comparable change in $2C + D$. The probe radius R, patch width A, and patch height T have no significant effect on the value of this resonance, again supporting the half wavelength slot mode hypothesis. Further study is required to capture more fully this resonant behavior over a larger variation of substrate permittivity and slot dimensions.

The Second Resonance $f_{\rm res2}$: The second resonant frequency f_{res2} is strongly related to the TM_{01} mode of the patch. However, this resonant frequency will be lower than that of the plain patch since the U-slot disturbs the usual current paths of the TM_{01} mode. As with $f_{\rm res1}$, $f_{\rm res2}$ does not change appreciably with different patch widths A and the current distribution on the patch surface does not have dominant currents in the x-direction. Indeed, simulation of the patch's surface currents shows a very high y-directed current distribution along the patch edges and on the outer edges of the arms of the U-slot, as also noted in [18]. The results of the parametric studies indicate that this resonant frequency depends most strongly on the length of the patch B and the length of the base of the U-slot D. D matters because it affects the apparent length of the current paths between the feed point and the two main radiating edges of the patch (Horizontal Top and Horizontal Bottom). The slope of the lines in Figs. 4 and 5 for $f_{\rm res2}$ indicate that the effect of B is twice as great as the effect of D, so that an approximate expression for the second resonance frequency can be given as

$$f_{\rm res2} \approx \frac{v_o}{2\sqrt{\varepsilon_{\rm eff}}\left(B + 2\Delta B + \frac{D}{2} - E\right)}. \quad (1)$$

Δ is also included in (1) to capture the effect of the new longer current paths created by the presence of the U-slot.

The Third Resonance $f_{\rm res3}$: The third resonance of the structure presents some interesting complexities that indicate the presence of both x-directed and y-directed resonant modes. First, the third resonance frequency $f_{\rm res3}$ reacts differently with increases of the U-slot base length D than the other frequencies. For certain ranges of C, increases in the value of D cause the third resonant frequency to increase (illustrated in Fig. 4). Since the currents from the feed point have a longer path around the U-slot to the Horizontal Bottom edge with increasing D, the frequencies at which a y-directed mode exist should decrease. This particular characteristic of $f_{\rm res3}$ indicates the existence of a mode in the x-direction of the patch since the only meaningful current paths getting shorter when D increases are those between the feed point and the Vertical Left and Vertical Right patch edges. The relatively large x-directed component in the antenna's current distribution and a corresponding level of cross polarization in the far-field radiation pattern at $f_{\rm res3}$ compared to that at other frequencies confirms this assertion. Others have also noted the high cross-polar radiation present at some frequencies within the operating bandwidth [18].

Behavior of this resonance with changes in C and A lends more credence to this hypothesis. With a constant horizontal slot length $D = 16$ mm and a decreasing vertical slot length C, $f_{\rm res3}$ increases toward the frequency of a TM_{20} patch mode. The cross-polarization level in the far-field increases as C decreases, with the cross-polar component being higher than the copolar component when $C = 0$ mm. Additionally, increases in the patch width A cause $f_{\rm res3}$ to shift downward significantly compared to all other resonant frequencies. This also indicates a TM_{20}-related mode.

Along with this x-directed mode that appears for some geometries, most antenna and slot combinations still exhibit a dominant y-directed mode. For instance, with long vertical slot lengths C, $f_{\rm res3}$ has stronger currents in the y-direction

TABLE IV
DIMENSIONS AND MATERIAL PROPERTIES OF DESIGN EXAMPLE 1

A [mm]	B [mm]	C [mm]	D [mm]	E [mm]	F [mm]	H [mm]	R [mm]	T [mm]	Offset [mm]	ε_r
70.6	42.6	23.3	25.9	2.3	2.3	10.0	0.64	6.35	0.0	2.20

than in the x-direction and has corresponding levels of co- and cross-polarization in the radiation pattern. The strongest y-directed currents are located on the inner edges of the vertical slot edges, in contrast to those at $f_{\rm res2}$, where the strongest y-directed currents are on outside of the U-slot. The parametric studies indicate that the antenna's behavior in the neighborhood of this resonance can be dominated by a y-directed mode if the ratio C/D is equal to or greater than 0.75 and the ratio C/A is equal to or greater than 0.30. Selection of the geometry to conform to these requirements will help to avoid the large cross-polar components in the radiation patterns noted by other researchers [18]. Therefore, the best approximation to the third resonant frequency (within roughly 10%) is given by the formula for the patch without the slot

$$f_{\rm res3} \approx \frac{v_0}{2\sqrt{\varepsilon_{\rm eff}}(B+2\Delta B)} \tag{2}$$

assuming that the ratios of C/D and C/A are controlled as discussed previously. The feed position will have an effect on the accuracy of this prediction but was not included in these parametric studies.

The Fourth Resonance $f_{\rm res4}$: The fourth resonant frequency $f_{\rm res4}$ is mainly the first resonant frequency of the slot in air, moderated by a y-directed resonance of the small pseudopatch formed inside the U-slot. This hypothesis is supported with the following reasoning and parametric study data. The fourth resonant frequency does not change appreciably with changes in patch length B, although this mode exhibits a large copolar field component in the far field. This leads to the conclusion that the resonance is strongly related to the slot. Further evidence of a slot mode is provided by the antenna's behavior with changes in slot dimensions. As D and C increase, the resonant frequency decreases. Moreover, as D increases, the copolar field component increases and the cross-polar component in the far-field decreases as one would expect for a radiating slot. However, numerical predictions of the slot's resonant frequency do not always match the simulation results of the complete antenna's fourth resonant frequency. The numerical data suggest that the geometry also supports the y-directed resonance of the small pseudopatch formed in the inside of the U that forms a hybrid mode with the slot resonance. Qualitative support for this hypothesis includes higher resonant frequencies for increased values of H. Quantitatively, the data in these parametric studies indicate that the fourth resonant frequency of the antenna can be approximated by the average of the first slot resonant frequency in air and the resonant frequency of the small pseudopatch formed inside the U-slot, that is

$$f_{\rm res4} \approx \frac{v_0}{(2C+D)+\sqrt{\varepsilon_{\rm eff(pp)}}(B-E-H+2\Delta_{B-E-H})}. \tag{3}$$

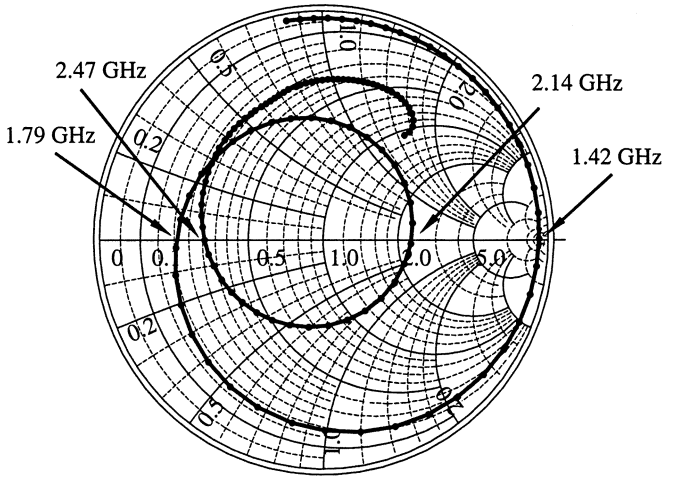

Fig. 6. Input impedance plot of Design Example 1 from 1.0 to 3.5 GHz, with the four resonant frequencies noted.

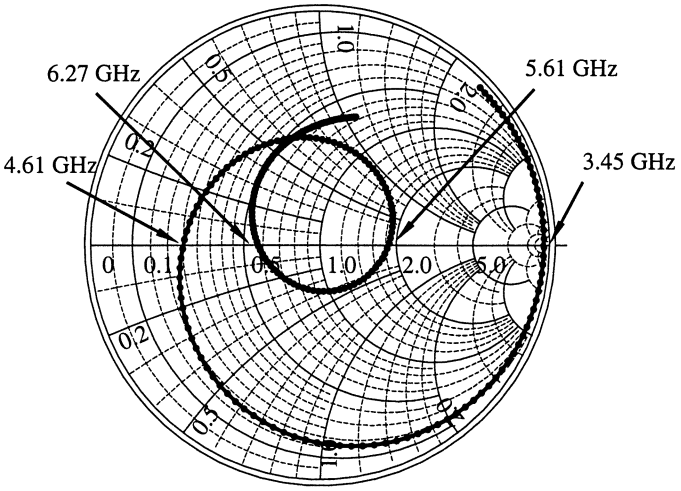

Fig. 7. Input impedance plot of Design Example 2 from 3.0 to 7.5 GHz, with the four resonant frequencies noted.

In (3), the effective permittivity of the pseudopatch $\varepsilon_{\rm eff(pp)}$ and the effective length extension $2\Delta_{B-E-H}$ are calculated with an effective patch width of $D-2F$. This hybrid mode hypothesis is by no means proven, however, since this hypothesis predicts larger changes in the resonant frequency with changes in B than were observed. Additionally, the parametric studies did not include a significant range of values of H (which determines slot position and therefore the length of the pseudopatch) for different slot geometries, so further investigation is warranted.

B. Summary

Table III summarizes the qualitative relationships between the antenna geometry and its critical properties. In the case of

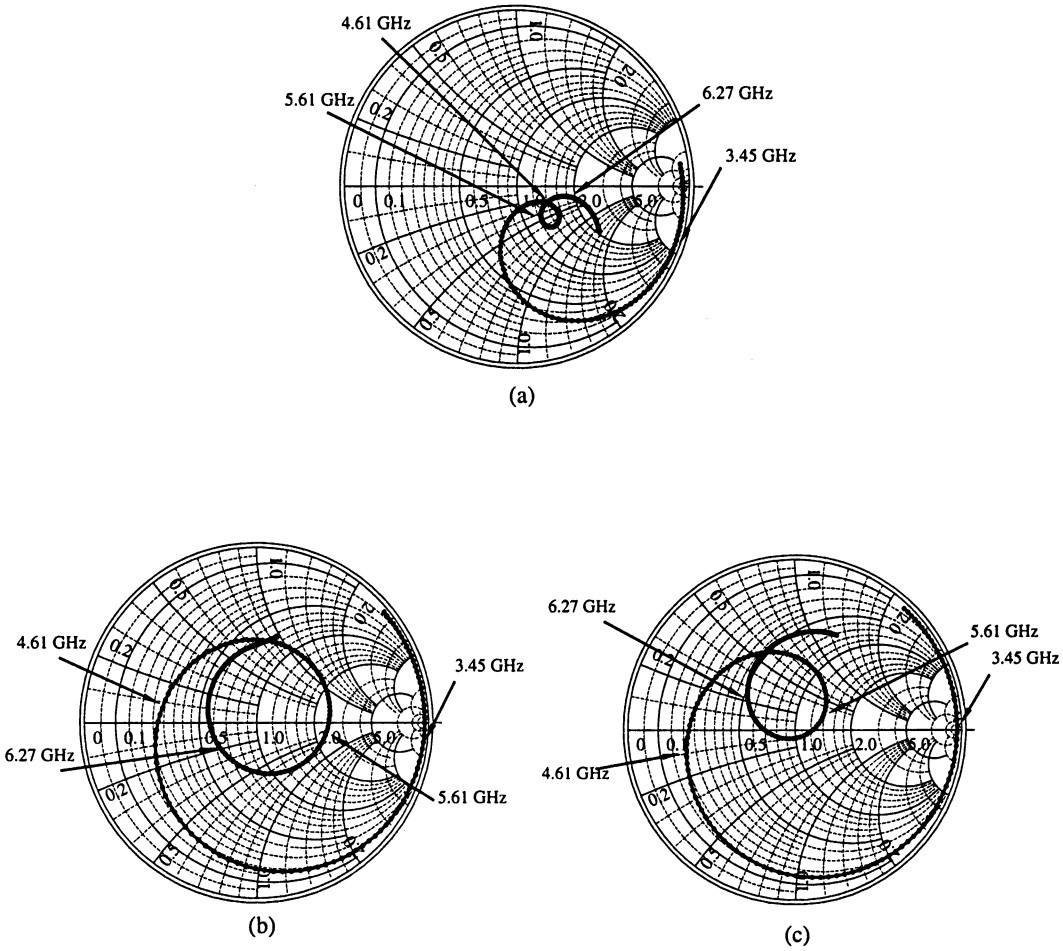

Fig. 8. Impedance plots of Design Example 2 from 3.0–7.5 GHz with (a) an increased substrate height; (b) a negative feedpoint offset; and (c) a positive feedpoint offset. Resonant frequencies of the original structure are designated for reference.

TABLE V
DIMENSIONS AND MATERIAL PROPERTIES OF DESIGN EXAMPLE 2

A [mm]	*B* [mm]	*C* [mm]	*D* [mm]	*E* [mm]	*F* [mm]	*H* [mm]	*R* [mm]	*T* [mm]	Offset [mm]	ε_r
26.6	15.4	9.3	12.0	0.8	0.8	4.5	0.3	3.175	0.0	2.20

the first resonant frequency $f_{\rm res1}$ none of the simulated geometries resulted in a VSWR ≤ 2. Table entries indicate how the increase of a geometric parameter affects the trend of the resonant frequencies and VSWR values. For example, an increase of the patch length ($B+$) decreases the first three resonant frequencies, $f_{\rm res1}$ to $f_{\rm res3}$, but does not affect $f_{\rm res4}$. A zero ("0") in Table III indicates that the behavioral parameter does not change appreciably with that geometry modification. When a "(+)" or "(−)" stands behind the "0" then a behavioral parameter change with that particular geometric change is much less significant than others. The comment "$*$" at $f_{\rm res3}$ is a reminder that the nature of the resonance changes with different ratios of C/A and C/D as discussed previously.

The rows "Δf_{12}," "Δf_{23}," "Δf_{34}," "Δf_{24}," and "Δf_{14}" indicate if two specific resonant frequencies move apart or together (for example at $\Delta f_{12} = f_{\rm res2} - f_{\rm res1}$, a "+" means that $f_{\rm res2}$ and $f_{\rm res1}$ move apart). The row "$|\Delta f_{34} - \Delta f_{23}|$" captures information about the location of the impedance loop relative to the real axis of the Smith chart (i.e., $|\Delta f_{34} - \Delta f_{23}| = 0$ indicates that the loop is in the vertical center of the Smith chart). The rows "VSWR$_2$," "VSWR$_3$" and "VSWR$_4$" in Table III display the relative changes of the VSWR values of the specific resonant frequencies (VSWR$_2$ is the VSWR-value at $f_{\rm res2}$). Additionally, "Δ VSWR$_{34}$," "Δ VSWR$_{23}$," "Δ VSWR$_{24}$" are the differences between the VSWR values at different resonant frequencies which may provide useful information if a designer wants to maintain VSWR$_2 \approx$ VSWR$_3 \approx$ VSWR$_4 < 2$ to ensure broad-band operation.

In some cases, changes in antenna parameters do not always move the VSWR of a resonant frequency in a single direction. That is, changes in some of the dimensions of the antenna cause the VSWR to decrease to a certain level and then increase. This happens, for example, to VSWR$_2$ when the slot gap widths, E and F, are steadily decreased. This behavior is indicated with a "v" in Table III. A "$\wedge$" is the opposite behavior of a "v." This phenomenon implies that a subset of antenna parameters can

TABLE VI
DIMENSIONS AND MATERIAL PROPERTIES OF DESIGN EXAMPLE 3

A [mm]	B [mm]	C [mm]	D [mm]	E [mm]	F [mm]	H [mm]	R [mm]	T [mm]	Offset [mm]	ε_r
19.0	10.2	6.6	6.0	0.6	0.6	2.0	0.3	3.175	0.0	2.20

be adjusted to achieve the "best" geometry for matching of a particular resonance.

III. DESIGN PROCEDURE

If an antenna designer wishes to develop an antenna design with specified characteristics, convergence to the desired functionality often requires a tradeoff between specific desired properties. For example, an overall improvement of an antenna's standing wave ratio will likely also decrease the frequency bandwidth and vice versa. To balance these tradeoffs and insure broad-band operation, we adopt the design strategy of keeping the VSWR at the resonant frequencies as close as possible and striving to achieve a nearly constant VSWR over the impedance bandwidth, creating a concentric circle on the Smith chart plot. Since the first resonance has a very high input resistance and would require an impedance transformer, this design procedure concentrates on the second, third, and fourth resonances of the structure to provide broad-band operation. To achieve a concentric circle in the horizontal center of the Smith chart, the difference between the second and third resonant frequency should be approximately equal to the difference between the third and the fourth resonant frequency, that is, $f_{\text{res3}} - f_{\text{res2}} \approx f_{\text{res4}} - f_{\text{res3}}$. Assuming that the VSWR at all of the resonant frequencies is less than 2, the antenna bandwidth (VSWR < 2) can be estimated by the frequency difference between the second resonant frequency f_{res2} and the fourth resonant frequency f_{res4} ($\Delta f_{24} = f_{\text{res4}} - f_{\text{res2}}$). Note, however, that nothing in the design procedure insures any value for the VSWR at any resonant frequency. This limitation is discussed more fully in Section IV.

This design procedure is based on the data and analysis of the parametric studies discussed earlier. The goal of this procedure is to provide a good first-pass design that can then be fine-tuned using the information in Table III.

1) Specify the center frequency and 2:1 VSWR bandwidth of the desired antenna. Approximate the center frequency as f_{res3} and the lower and upper frequency bounds of the bandwidth as f_{res2} and f_{res4}, respectively.
2) Select a substrate permittivity ε_r and a substrate thickness T. There is a lower limit on T below which broad-band operation is unlikely. Therefore, the substrate thickness and permittivity should satisfy the following rule of thumb derived from the existing literature and the parametric studies

$$T \geq 0.06 \frac{\lambda_{\text{res3}}(air)}{\sqrt{\varepsilon_r}}.$$

3) Estimate the quantity $B + 2\Delta B$ as follows

$$B + 2\Delta B \approx \frac{v_0}{2\sqrt{\varepsilon_r} f_{\text{res3}}}.$$

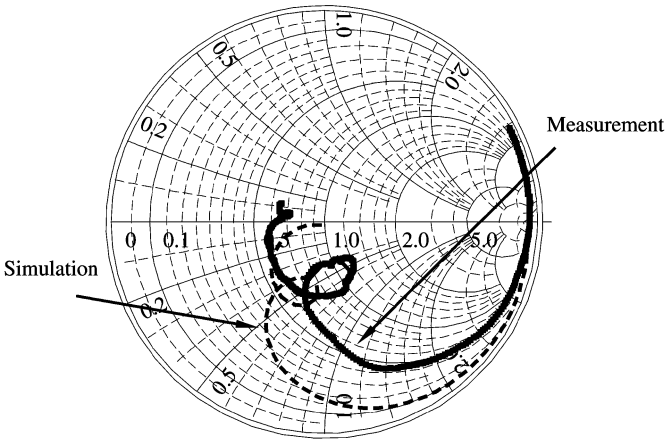

Fig. 9. Design Example 3 measured and simulated impedance plot from 5.0–10.0 GHz.

4) Calculate A as

$$A = 1.5(B + 2\Delta B).$$

5) Calculate ε_{eff} and $2\Delta B$ using the following common equations found in [27] and [28], respectively:

$$\varepsilon_{\text{eff}} = \frac{\varepsilon_r + 1}{2} + \frac{\varepsilon_r - 1}{2}\left(1 + \frac{12T}{A}\right)^{-1/2}$$

$$2\Delta B = 0.824T \frac{(\varepsilon_{\text{eff}} + 0.3)\left(\frac{A}{T} + 0.262\right)}{(\varepsilon_{\text{eff}} - 0.258)\left(\frac{A}{T} + 0.813\right)}.$$

6) Backcalculate the value of B

$$B = \frac{v_0}{2\sqrt{\varepsilon_{\text{eff}}} f_{\text{res3}}} - 2\Delta B.$$

7) Select a starting value of slot thickness using the following rule of thumb:

$$E = F = \frac{\lambda_{\text{res3}}(air)}{60}.$$

8) Calculate D by solving (1)

$$D = \frac{v_0}{\sqrt{\varepsilon_{\text{eff}}} f_{\text{res2}}} - 2\left(B + 2\Delta B - E\right).$$

9) Select C such that

$$\frac{C}{A} \geq 0.3 \quad \text{and} \quad \frac{C}{D} \geq 0.75.$$

10) Calculate the effective permittivity and effective length extension of the pseudopatch of the fourth resonance with the effective patch width as $D - 2F$

$$\varepsilon_{\text{eff(pp)}} = \frac{\varepsilon_r + 1}{2} + \frac{\varepsilon_r - 1}{2}\left(1 + \frac{12T}{D - 2F}\right)^{-1/2}$$

$$2\Delta_{B-E-H} = 0.824T \frac{\left(\varepsilon_{\text{eff(pp)}} + 0.3\right)\left(\frac{D-2F}{T} + 0.262\right)}{\left(\varepsilon_{\text{eff(pp)}} - 0.258\right)\left(\frac{D-2F}{T} + 0.813\right)}.$$

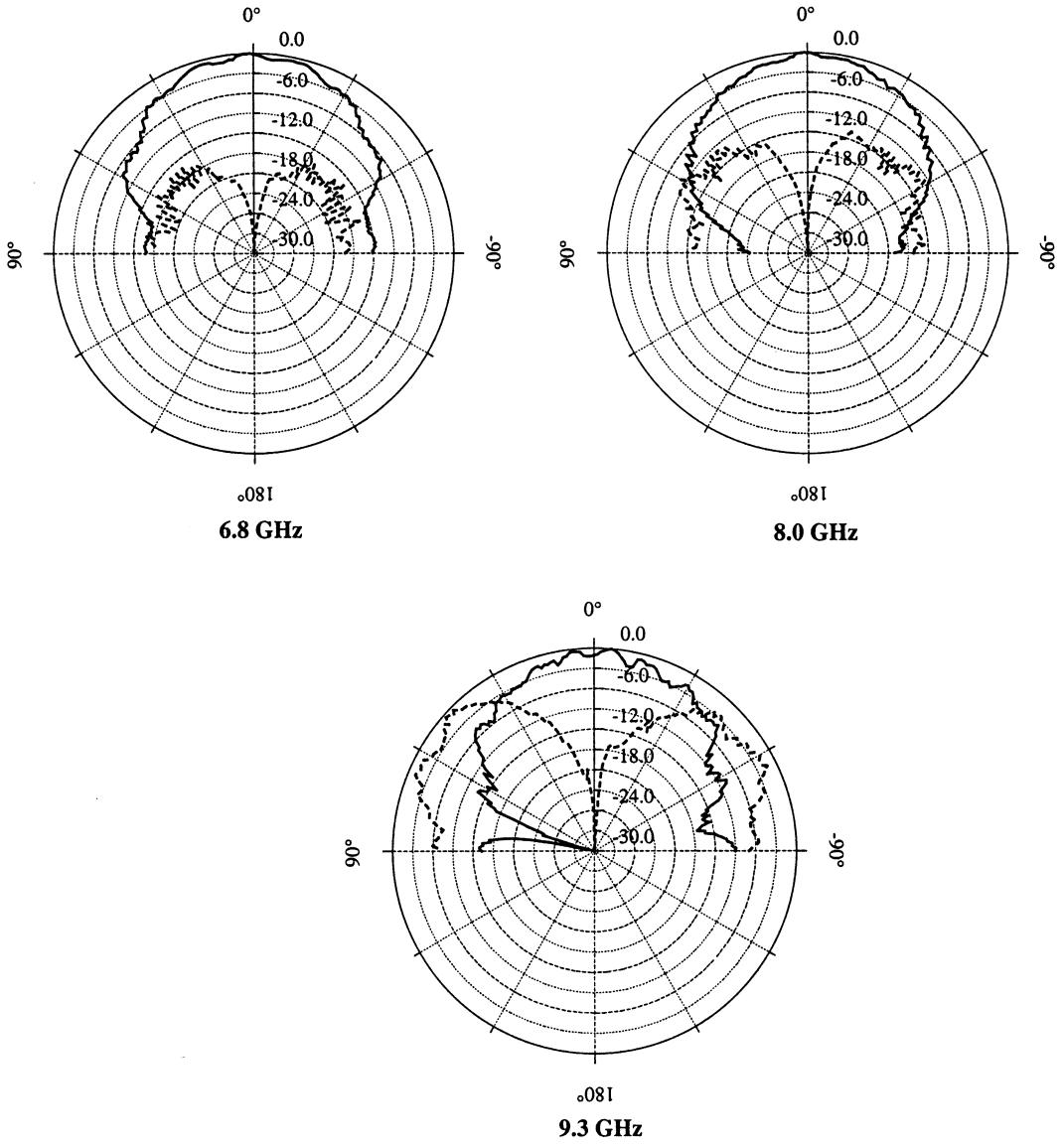

Fig. 10. Normalized measured H plane radiation patterns of Design Example 3 in dB for three operating frequencies. (— copolar, - - - crosspolar). As the operating frequency increases, the copolar and cross-polar levels become comparable.

11) Calculate H by solving (3):

$$H \approx B - E + 2\Delta_{B-E-H} - \frac{1}{\sqrt{\varepsilon_{\mathrm{eff(pp)}}}}\left(\frac{v_0}{f_{\mathrm{res4}}} - (2C + D)\right).$$

12) Check that the sum $C + E + H$ is less than B. If not, adjust C by changing the ratios in Step 9 and the value of H until the design is physically realizable.

IV. Design Examples

This section provides three antenna designs to illustrate the capabilities and shortcomings of the procedure outlined in Section III. In each design, the percentage bandwidth is calculated by dividing the frequency bandwidth defined by a VSWR of 2 or less by the center frequency defined as the arithmetic mean of the VSWR $= 2$ frequencies of the band. The first design is intended to cover both the PCS and WLAN communication bands from 1.8–2.0 GHz and 2.4–2.5 GHz, respectively. Note that using a broad-band rather than a dual band design for this application may not be advisable in practice. The 2 : 1 frequency bandwidth is specified from 1.8–2.5 GHz, with a center frequency of 2.15 GHz. This translates to a 32% bandwidth. Following the design procedure, the 2.15 GHz is specified as f_{res3} and 1.8 and 2.5 GHz are specified as f_{res2} and f_{res4}, respectively. A substrate with a permittivity of 2.2 and a height equal to 6.35 mm is chosen to satisfy the requirements in Design Step 2. Following the remaining steps with a selection of $C/A = 0.33$ and $C/D = 0.9$ yields the dimensions provided in Table IV. The simulated input impedance of this design is shown in Fig. 6. The first resonance is predicted to be 1.39 GHz, and the simulation shows a resonant frequency of 1.42 GHz. The simulated second, third, and fourth resonant frequencies (1.79, 2.14, 2.47 GHz) are also very close to the design goals of 1.77, 2.15, and 2.54 GHz, respectively. This example demonstrates that while the design procedure can do a good job of producing an antenna with designated resonant frequencies, it does not necessarily give a design with good bandwidth characteristics, which are still largely a

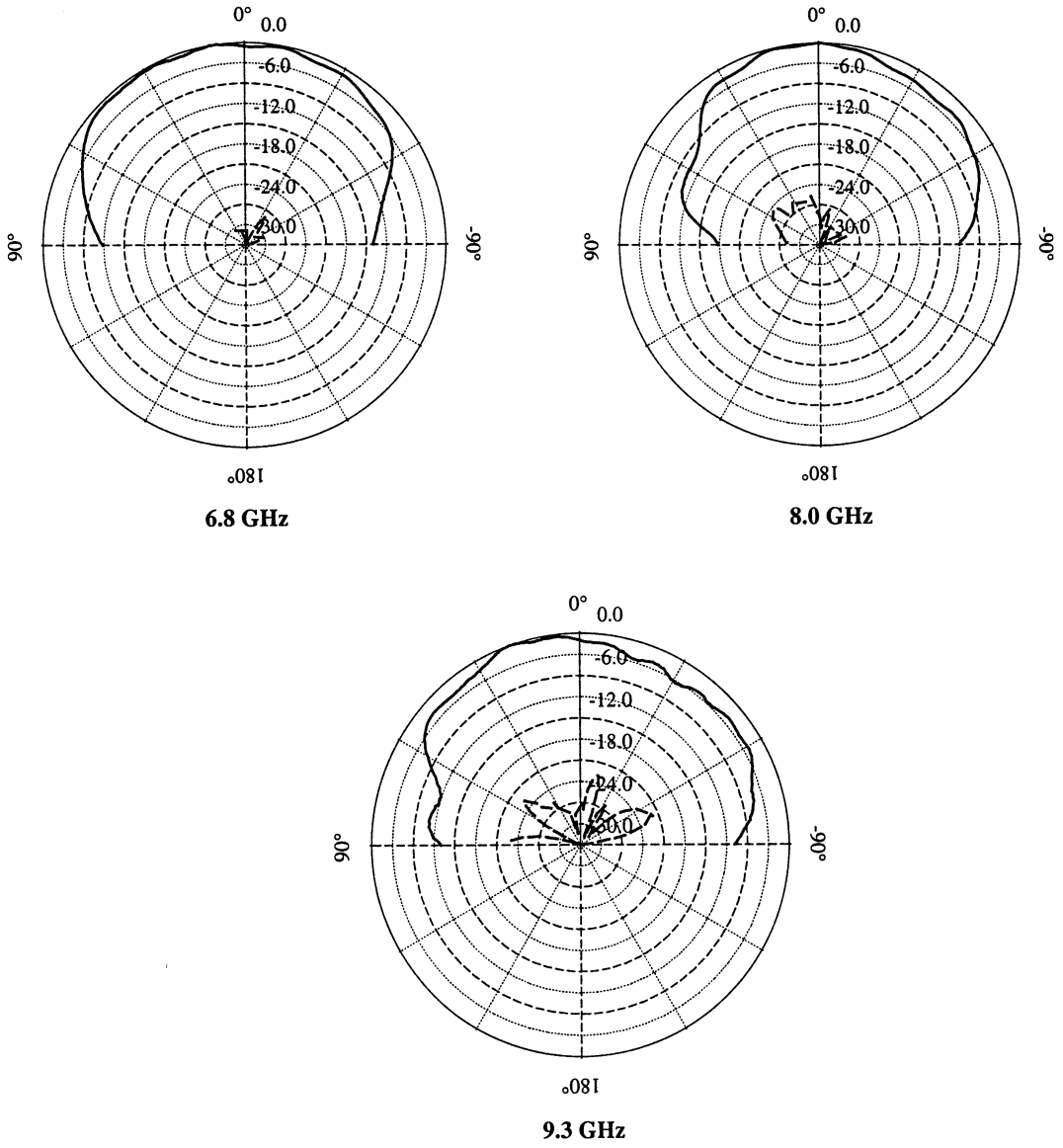

Fig. 11. Normalized measured E plane radiation patterns of Design Example 3 in dB for three operating frequencies. (— copolar, - - - crosspolar).

function of dielectric thickness and feed point position. Indeed, the VSWR of this antenna never falls below 2.

A second example helps to illustrate the effects of changes in substrate thickness and feed point position and provides guidance for tuning the first pass designs provided by the design procedure. The preliminary design parameters for this antenna are given in Table V. According to the design procedure, this antenna should have the first, second, third, and fourth resonant frequencies at 3.30, 4.46, 5.71, and 6.61 GHz, respectively. If the 2 : 1 VSWR bandwidth were defined by the second and fourth resonant frequencies, the antenna would have a 39% bandwidth. Fig. 7 presents the simulated impedance response of this antenna from 3.0 to 7.5 GHz, which indicates a 15% bandwidth centered around 5.97 GHz. Fig. 8 demonstrates the effects of several changes to this initial design. Except for each of these changes, the geometrical parameters of the antenna given in Table VI remain the same. Fig. 8(a) depicts the effects of a change in the height of the substrate to 6.35 mm and a probe radius of 0.615 mm, resulting in a 2 : 1 VSWR between 4.21 and 6.26 GHz that corresponds to a 5.24 GHz center frequency with a 39% bandwidth. Fig. 8(b) shows the change of a small negative shift in the feed point position, resulting in a 2 : 1 VSWR between 5.84 and 6.66 GHz that corresponds to a 6.25 GHz center frequency with a 13% bandwidth. Fig. 8(c) shows the change of a small positive shift in the feed point position, resulting in a 2 : 1 VSWR between 5.44 and 6.23 GHz that corresponds to a 5.84 GHz center frequency with a 13.5% bandwidth. Using this information, a combination of the substrate and feed point position changes can be determined to produce a design with a broad-band characteristic for the specified band. In the tuning procedure, dramatic changes in substrate height will often produce a dual-band rather than a single broad-band characteristic that then may be shifted on the Smith chart by movement of the feed point position. In some cases, changes in these two variables alone will not be enough to completely tune the antenna and other variables, including C, E, F, and H, can be used to arrive at the desired antenna response.

The third design is selected to provide a 2 : 1 VSWR bandwidth between 6.6 GHz and 9.0 GHz with a third resonant frequency of 8.0 GHz. Using a substrate with a relative permittivity of 2.2 and a thickness of 3.175 mm, the ratios C/A and C/D are selected to be 0.35 and 0.92, respectively. Antenna dimensions are provided in Table VI. The simulated and measured input impedances of this design are shown in Fig. 9. In this case, the loop on the Smith chart does not cross the real axis to indicate true resonant frequencies, but the VSWR of this antenna is less than 2 : 1 from 6.86 to 9.88 GHz, which is a much larger impedance bandwidth than intended. Measurements of the antenna's radiation patterns (Figs. 10 and 11) indicate that as the frequency approaches 9.3 GHz, the level of copolar and crosspolar fields become comparable in the H plane, indicating that the actual useful bandwidth of the antenna is closer to the design specification than the measured impedance bandwidth implies (assuming that linear polarization with a low cross-polar component is desired).

V. Conclusion and Future Outlook

This paper presents a new design procedure for the U-slot rectangular patch antenna based on previous literature and theoretical and parametric analyses. The origins of the structure's multiple resonant frequencies, which can be combined to produce a broad-band frequency response, are analyzed and discussed. Approximate formulas are introduced to describe these resonant frequencies that are then implemented in the design of new antennas. Results of parametric studies are provided to aid in the fine-tuning of preliminary designs. Several new antennas are designed using the outlined procedure and evaluated with simulations and measurements. While the design rules presented here are approximate and may not work in all situations, they do provide an excellent starting point for antenna designers that give better and more timely results than simple guesses or cut-and-try techniques.

Further study is necessary in several areas to arrive at a more complete picture of this antenna's capabilities. Clearly, the substrate thickness and the feed point position remain important factors in achieving broad-band frequency operation [10] and further parametric studies on these variables, as well as U-slot position and coaxial probe radius, are required. Second, these additional studies need to be coupled with the present paper and more detailed theoretical examinations to determine if some geometric factors can be used to compensate mismatches caused by prespecified substrate heights and probe radii. Finally, this paper can be used as a basis to derive design techniques for similar structures that result in multiband rather than broad-band operation.

Acknowledgment

The authors would like to thank Rogers Corporation for providing the dielectric substrate material.

References

[1] R. Q. Lee, K. F. Lee, and J. Bobinchak, "Characteristics of a two-layer electromagnetically coupled rectangular patch antenna," *Electron. Lett.*, vol. 23, no. 20, pp. 1070–1072, 1987.

[2] W. Chen, K. F. Lee, and and R. Q. Lee, "Spectral-domain moment-method analysis of coplanar microstrip parasitic subarrays," *Microw. Opt. Technol. Lett.*, vol. 6, no. 3, pp. 157–163, 1993.

[3] K. H. Pan, J. T. Bernhard, and T. Moore, "Effects of lossy dielectric materials on microstrip antennas," in *Proc. IEEE AP-S Conf. Antennas and Propagation for Wireless Communications*, Nov. 2000, pp. 39–42.

[4] J. T. Aberle, M. Chu, and C. R. Birtcher, "Scattering and radiation properties of varactor-tuned microstrip antennas," in *IEEE Antennas Propagat. Soc. Int. Symp. Digest*, vol. 4, 1992, pp. 2229–2232.

[5] K. Guney, "Resonant frequency of a tunable rectangular microstrip patch antenna," *Microw. Opt. Tech. Lett.*, vol. 7, no. 12, pp. 581–585, Aug. 20, 1994.

[6] S.-C. Pan and K. L. Wong, "Dual-frequency triangular microstrip antenna with a shorting pin," *IEEE Trans. Antennas Propagat.*, vol. 45, pp. 1889–1891, Dec. 1997.

[7] T. Huynh and K. F. Lee, "Single-layer single-patch wideband microstrip antenna," *Electron. Lett.*, vol. 31, no. 16, pp. 1310–1312, Aug. 3, 1995.

[8] K. F. Lee, K. M. Luk, K. F. Tong, Y. L. Yung, and T. Huynh, "Experimental study of the rectangular patch with a U-shaped slot," in *IEEE Antennas Propagat. Soc. Int. Symp. Digest*, vol. 1, 1996, pp. 10–13.

[9] K. F. Tong, K. M. Luk, K. F. Lee, and S. M. Shum, "Analysis of broadband U-slot microstrip antenna," in *IEE Tenth Int. Conf. Antennas Propagat.*, vol. 1, 1997, pp. 110–113.

[10] K. F. Lee, K. M. Luk, K. F. Tong, S. M. Shum, T. Huynh, and R. Q. Lee, "Experimental and simulation studies of the coaxially fed U-slot rectangular patch antenna," in *Inst. Elect. Eng. Proc.-Microw. Antennas Propagat.*, vol. 144, Oct. 1997, pp. 354–358.

[11] Y. L. Chow and K. H. Shiu, "A theory on the broadbanding of a patch antenna," in *Asia-Pacific Microwave Conf. Proc.*, vol. 1, 1997, pp. 245–248.

[12] K. M. Luk, K. F. Tong, S. M. Shum, K. F. Lee, and R. Q. Lee, "FDTD analysis of U-slot rectangular patch antenna," in *IEEE Antennas Propagat.Society Int. Symp. Digest*, vol. 4, 1997, pp. 2111–2114.

[13] K. F. Tong, K. M. Luk, and K. F. Lee, "Design of a broadband U-slot patch antenna on a microwave substrate," in *Asia-Pacific Microwave Conf. Proc.*, vol. 1, 1997, pp. 221–224.

[14] Y. L. Chow and C. W. Fung, "The City University logo patch antenna," in *Asia-Pacific Microwave Conf. Proc.*, vol. 1, 1997, pp. 229–232.

[15] A. A. Omar, "Efficient analysis of a U-slot patch antenna using contour integral method with complex images," in *IEEE Antennas Propagat. Soc. Int. Symp. Digest*, vol. 3, 1998, pp. 1602–1605.

[16] Y. L. Chow, Z. N. Chen, K. F. Lee, and K. M. Luk, "A design theory on broadband patch antennas with slot," in *IEEE Antennas Propagat. Soc. Int. Symp. Digest*, vol. 2, 1998, pp. 1124–1127.

[17] Y. X. Guo, K. M. Luk, K. F. Lee, and Y. L. Chow, "Double U-slot rectangular patch antenna," *Electron. Lett.*, vol. 34, no. 19, pp. 1805–1806, Sept. 17, 1998.

[18] M. Clenet and L. Shafai, "Multiple resonances and polarization of U-slot patch antenna," *Electron. Lett.*, vol. 35, no. 2, pp. 101–103, Jan. 21, 1999.

[19] K. M. Luk, K. F. Lee, and W. L. Tam, "Circular U-slot patch with dielectric superstrate," *Electron. Lett.*, vol. 33, no. 12, pp. 1001–1002, June 5, 1997.

[20] Y. X. Guo, K. M. Luk, and K. F. Lee, "U-slot circular patch antennas with L-probe feeding," *Electron. Lett.*, vol. 35, no. 20, pp. 1694–1695, Sept. 30, 1999.

[21] S. Y. Rhee, G. H. Lee, J. T. Ihm, and Y. H. Lee, "Experimental study of a microstrip-probe feed for U-slot patch array antennas," in *IEEE Antennas Propagat. Soc. Int. Symp. Digest*, vol. 4, 1999, pp. 2756–2759.

[22] J. Rosa, R. Nunes, A. Moleiro, and C. Peixeiro, "Dual-band microstrip patch antenna element with double U slots for GSM," in *IEEE Antennas Propagat. Soc. Int. Symp. Digest*, vol. 3, 2000, pp. 1596–1599.

[23] F. Tavakkol-Hamedani, A. Tavakoli, and L. Shafai, "Analysis of Yagi-Uda, U-slot and shorted finite microstrip antennas using surface equivalence principle and multiple network theory (SEMN)," in *IEEE Antennas Propagat. Soc. Int. Symp. Digest*, vol. 2, 2000, pp. 852–855.

[24] K. F. Tong, K. M. Luk, K. F. Lee, and R. Q. Lee, "A broad-band U-slot rectangular patch antenna on a microwave substrate," *IEEE Trans. Antennas Propagat.*, vol. 48, pp. 954–960, June 2000.

[25] Zeland Software Inc., *IE3D User's Manual* Fremont, CA, 1999, Release 7.

[26] I. J. Bahl and P. Bhartia, *Microstrip Antennas*. Dedham, MA: Artech House, 1982, (second printing).

[27] R. P. Owens, "Accurate analytical determination of quasistatic microstrip line parameters," *The Radio and Electronic Engineer*, vol. 46, no. 7, pp. 360–364, July 1976.

[28] E. O. Hammerstad, "Equations for microstrip circuit design," in *Proc. Fifth Europ. Microwave Conf.*, Sept. 1975, pp. 268–272.

Steven Weigand (S'00–M'01) was born in Freising, Germany, in 1974. He received the Dipl.Ing. (M.Sc.) degree in electrical engineering from the Technical University of Darmstadt, Darmstadt, Germany, in 2001.

In 2000, he worked as a visiting researcher with the Department of Electrical Engineering and Computer Engineering, the University of Illinois at Urbana-Champaign. He was involved in the research and development of broad-band patch antennas. In 2001, he joined WJ Communications Inc., San Jose, CA, where he is an RF design engineer. His current research interests include antennas, MMICs, and wireless transceivers.

Greg H. Huff was born in Oklahoma City, OK, on April 16, 1975. He received the B.S.E.E. degree from the University of Illinois at Urbana-Champaign (UIUC) in 2001.

He is currently pursuing the Master's degree as a research assistant in the Electromagnetics Laboratory. Prior to his continuing education at UIUC, he apprenticed and worked as a chef in the eastern and midwest region of the United States for several years. His current research involves thin film para/ferroelectrics in multilayer tunable microwave and millimeter wave devices and reconfigurable antennas, as well as electromagnetic compatibility and packaging of high-frequency devices.

Kankan H. Pan received the B.S. degree in computer science from Beijing Polytechnic University, and the M.S. degree in electrical engineering from the University of Illinois at Urbana-Champaign, in 1996 and 2001 respectively.

She is currently an electrical engineer with Agilent Technologies, Santa Rosa, CA, where she is engaged in the development of high-performance spectrum analyzers. Her interests include RF circuits and microstrip antenna design.

Jennifer T. Bernhard (S'89–M'95–SM'01) was born on May 1, 1966, in New Hartford, NY. She received the B.S.E.E. degree from Cornell University, Ithaca, NY, in 1988. While at Cornell, she was a McMullen Dean's Scholar and participated in the Engineering Co-op Program at IBM Federal Systems Division, Owego, NY. She received the M.S. and Ph.D. degrees in electrical engineering from Duke University in 1990 and 1994, respectively, with support from a National Science Foundation Graduate Fellowship.

During the 1994–1995 academic year, she held the position of Postdoctoral Research Associate with the Departments of Radiation Oncology and Electrical Engineering at Duke University, where she developed RF and microwave circuitry for simultaneous hyperthermia (treatment of cancer with microwaves) and MRI (magnetic resonance imaging) thermometry. At Duke, she was also an organizing member of the Women in Science and Engineering (WISE) Project, a graduate student-run organization designed to improve the climate for graduate women in engineering and the sciences. From 1995 to 1999, she was an Assistant Professor with the Department of Electrical and Computer Engineering at the University of New Hampshire, where she held the Class of 1944 Professorship. Since 1999, she has been an Assistant Professor with the Department of Electrical and Computer Engineering at the University of Illinois at Urbana-Champaign. In 1999 and 2000, she was a NASA-ASEE Summer Faculty Fellow with NASA Glenn Research Center, Cleveland, OH. Her industrial experience includes work as a research engineer with Avnet Development Labs and, more recently, as a private consultant for members of the wireless communication community. Her research interests lie in the areas of high-speed wireless data communication, reconfigurable microwave antennas and circuits, electromagnetic compatibility, and electromagnetics for industrial and medical applications.

Prof. Bernhard received the NSF CAREER Award in 2000. She is a member of Tau Beta Pi, Eta Kappa Nu, and Sigma Xi.